Progress In Electromagnetics Research B, Vol. 49, 389–409, 2013

AN IMPROVED ANALYTICAL MODEL FOR SALIENT POLE SYNCHRONOUS MACHINES UNDER GENERAL ECCENTRICITY FAULT

Hamidreza Akbari*

Department of Electrical Engineering, Yazd Branch, Islamic Azad University, Yazd, Iran

Abstract—This paper develops a more precise analytical model for calculating salient pole synchronous machine (SPSM) inductances in case of general eccentricity including static, dynamic and mixed eccentricities. The developed method is based on the modified winding function approach (MWFA) which accurately considers variable air gap function and leads to pure analytical expressions of inductances. Available analytical techniques, based on MWFA, approximate the air gap function and simplify the geometrical model of SPSM, whereas, in this study, the influence of the openings between the rotor salient poles has been taken into account by using an effective form of rotor pole shoes. Using this technique, flux fringing effect is considered. By taking into account machine geometry, type of windings connection and flux fringing effect, this method is able to model most of the important features of an eccentric SPSM. The developed analytical expressions can calculate time varying inductances of SPSMs with any eccentricity type and degree in the frame of a single program. Simulation results for static eccentricity are compared with experimental tests on a laboratory generator to verify accuracy of the proposed model.

1. INTRODUCTION

To model electrical machines under different types of faults, winding function approach (WFA) [1] and finite element method (FEM) [2] have been introduced as appropriate modeling methods. Although FEM provides precise modeling, its application is complicated and time consuming especially for the analysis of electrical machines with asymmetry in the motor body such as eccentricity [2, 3].

Received 1 January 2013, Accepted 5 March 2013, Scheduled 7 March 2013

* Corresponding author: Hamidreza Akbari (hamid_r_akbari@yahoo.com).

WFA is based on the basic geometry and winding layout of machine [1]. By this approach, it is possible to analyze the behavior of any machine with any winding distribution and air gap length. Hence this method has gained a broad application in the analysis of faulty electrical machines, such as broken rotor bars [4] and fault condition in stator windings [5].

Analysis of electrical machines with non-uniform air gap using WFA was not accurate until MWFA was proposed [6]. This theory has been applied to analyze static, dynamic and mixed eccentricity in induction and synchronous machines [7–9]. In [10], MWFA was extended for radial and axial non-uniform air gap in SPSMs.

An essential step of this approach is the calculation of machine inductances. An accurate inductances calculation is necessary to improve the accuracy of the analysis of electrical machines. In [12], an analytical equation of the air gap for an eccentric SPSM was presented. The inductances have been calculated by expressing the turn functions and inverse air-gap function in their Fourier series expansions. A numerical integration has been used to determine the values of inductances.

In the previous works, based on winding function theory, the calculation of SPSM inductances is carried out using numerical integration or inexact analytical equations based on approximated Fourier series expansions of the inverse air gap function [11–16], except [17], in which, the air gap function has been estimated by a step function.

In the present paper, more realistic inverse air-gap function of an eccentric SPSM is used to derive pure analytical expressions for inductances without any development in Fourier series. This will ensure that all space harmonics ignored by the Fourier series expansions of the inverse air gap function are included in the model. The influence of the flux fringing effect on the air gap function has been taken into account by using an effective air gap function. This results an increase in the accuracy of calculating machine inductances.

To the best of our knowledge, this is the first study for developing analytical method for calculation of SPSM inductances under different kinds of eccentricities, considering flux fringing effect, without any development in Fourier series. It is clear that the proposed technique decreases the time and computation process and leads to more accurate results.

To develop analytical expressions for inductances, the effective inverse air gap function of the eccentric SPSM has been defined, and its indefinite integral has then been determined. Developed analytical expressions make it possible to calculate inductances of SPSM with

any eccentricity type and degree in the frame of a single program. By using the presented method, inductances of a SPSM with eccentric rotor are calculated. The effects of several rotor asymmetries on the inductances are shown and the inductances are evaluated. Theoretical fundamentals and experimental results that validate the proposed technique are presented. Simulation results show that the result with proposed method is closer to the experimental result than that of available analytical methods.

The contributions of the present paper includes: 1) Defining the inverse air gap function of the eccentric SPSM and determining its indefinite integral, taking into account the flux fringing effect and 2) Developing a new closed form analytical expression for calculation of SPSM inductances under different types of eccentricities, using more realistic air gap function.

2. ECCENTRICITY MODELING

When eccentricity fault occurs in an electrical machine, three geometric centers; stator (o_s), rotor (o_r) and rotor rotation (o_c) don't coincide with each other.

There are three types of air-gap eccentricity: static, dynamic and mixed eccentricity [8]. Static eccentricity (SE) occurs when the rotor rotates about its own centerline, but this centerline does not coincide with that of the stator bore. Dynamic eccentricity (DE) occurs when the rotor geometric center is not at the center of rotation, producing an air-gap periodic variation as a rotor position function. In mixed eccentricity (ME) both rotor geometric center and the center of rotation are displaced individually in respect to the stator geometric center. Figure 1 shows an elementary SPSM for three types of eccentricities.

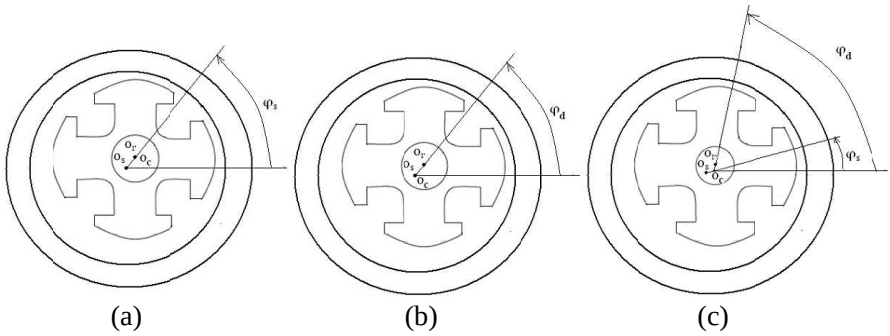

Figure 1. Different kinds of eccentricities in a SPSM. (a) SE, (b) DE, and (c) ME.

The air gap length variation under ME for an induction machine can be described by air gap function as follows [18]:

$$g(\varphi, \varphi_m, \delta) = g_0 \left(1 - \delta \cos\left(\varphi - \varphi_m\right)\right) \tag{1}$$

where

$$\delta = \left[\delta_s^2 + \delta_d^2 + 2\delta_s\delta_d \cos\left(\theta - \varphi_s\right)\right]^{1/2} \tag{2}$$

$$\varphi_m = \varphi_s + \tan^{-1}\left(\frac{\delta_d \sin(\theta - \varphi_s)}{\delta_s + \delta_d \cos\left(\theta - \varphi_s\right)}\right) \tag{3}$$

where, g_0 is air gap length for healthy machine, θ the rotor position angle in stator reference frame, φ the angle in stator reference frame, φ_s the angle at which rotation and stator centers are separated, and δ_s and δ_d are static and dynamic eccentricity levels, respectively.

These relations are used in the following section for developing analytical expressions of inductances of eccentric SPSM.

3. ANALYTICAL EQUATIONS OF INDUCTANCES FOR GENERAL ECCENTRICITY

According to MWFA, mutual inductance between two windings a and b in electrical machines, can be calculated by the following equation [6]:

$$L_{ab} = \mu_0 lr \int_0^{2\pi} n_a \cdot M_b \cdot g^{-1} d\varphi \tag{4}$$

where

$$M_b = n_b - \left(\int_0^{2\pi} g^{-1} \cdot n_b d\varphi\right) \Big/ \left(\int_0^{2\pi} g^{-1} d\varphi\right) \tag{5}$$

μ_0 is the free space permeability, l the axial stack length of the machine, g^{-1} the inverse air gap function, n_a the turns function of winding a, and M_b the modified winding function of winding b.

Available analytical methods for calculation of inductances of eccentric SPSM are based on the winding function theory. Although available analytical methods provide good knowledge about performance of eccentric SPSM, they are based on simplification and geometrical approximation of unsymmetrical models of the machine under different eccentricities. In [12], the values of inductances of an eccentric SPSM have been determined using Fourier series expansions of the inverse air gap function and numerical integration. In the recent studies [17, 20], analytical expressions have been presented assuming

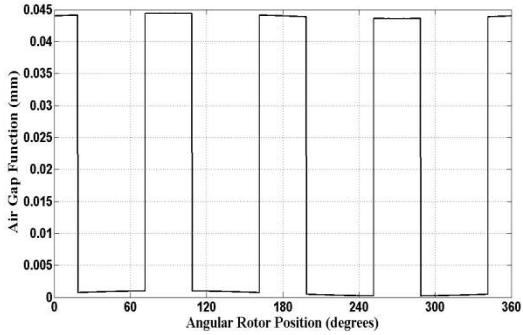

Figure 2. Approximated air gap function for a four pole eccentric SPSM (SE = 30%).

step function (Figure 2) for air gap distribution. In the present paper, effective air gap function which considers flux fringing effect is used to develop analytical expressions without any development in Fourier series.

To derive analytical expressions for inductances, the varying air gap length, due to the pole saliency, eccentricity and slots should first be modeled.

The influence of the pole saliency, can be taken into account by using the effective pole opening distance. The effective opening between the poles is slightly larger than the actual opening due to flux fringing. The air-gap function is computed by modeling the flux paths through the air-gap regions using straight lines and circular arc segments. The details of air gap function modeling in a salient pole synchronous machine considering flux fringing effect have been given in [19].

Knowing the actual opening and air gap length, the effective opening is calculated as [19]:

$$O' = \frac{\gamma}{\beta} g \tag{6}$$

where

$$\begin{aligned} \beta &= \frac{(1-u)^2}{2(1+u^2)} \\ u &= \frac{o}{2g} + \sqrt{1+\left(\frac{o}{2g}\right)^2} \\ \gamma &= \frac{4}{\pi}\left(\frac{o}{2g}\tan^{-1}\frac{o}{2g} - \ln\sqrt{1+\left(\frac{o}{2g}\right)^2}\right) \end{aligned} \tag{7}$$

where, o is the actual opening length. The effective air gap length within the effective pole opening, for a healthy SPSM can be expressed as

$$g_{eff}(\phi) = \frac{g}{1 - \beta\left(1 - \cos\frac{2\pi}{o'}\varphi\right)} \tag{8}$$

The eccentricity can be taken into account according to (1). Therefore, the effective air gap length of an eccentric SPSM, in interpolar space, can be described by air gap function as follows

$$g_q(\varphi, \varphi_m, \delta) = \frac{g_0\left(1 - \delta\cos\left(\varphi - \varphi_m\right)\right)}{1 - \beta\left(1 - \cos\frac{2\pi}{o'}\varphi\right)} \tag{9}$$

Elsewhere, in polar space, the air gap length is

$$g_d(\varphi, \varphi_m, \delta) = g_0(1 - \delta\cos(\varphi - \varphi_m)) \tag{10}$$

The subscripts d and q refer to the polar and interpolar regions, respectively.

In the case of static eccentricity, $\delta = \delta_s$ and $\varphi_m = \varphi_s$ and in dynamic eccentricity $\delta = \delta_d$ and $\varphi_m = \varphi_d$. In mixed eccentricity, both δ and φ_m are rotor position dependent as (2) and (3). Therefore we can define air gap function for SPSM with a general eccentricity fault, including static, dynamic and mixed eccentricities.

Figure 3 shows the effective air gap length for a four pole SPSM under 30% SE condition. This effective function is used in the present study for developing analytical equations.

Finally, the stator slots effect is taken into account by Carters' factor referred to the slots [19].

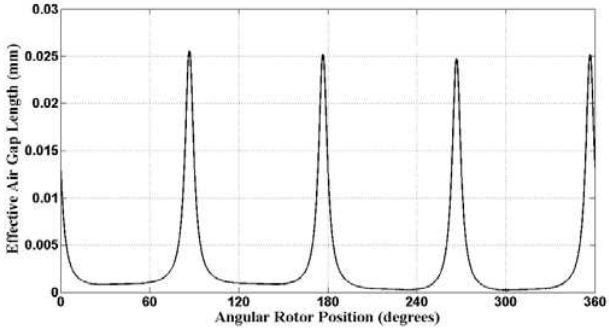

Figure 3. Effective air gap length for a four pole eccentric SPSM (for example: SE = 30%) used in this study for developing analytical equations.

3.1. Inductances of Stator Phases

To derive the analytical equations for inductances of stator phases, it is assumed that the functions y_d and y_q are indefinite integrals as follows

$$y_d(\varphi, \varphi_m, \delta) = \int g_d^{-1}(\varphi, \varphi_m, \delta) d\varphi \tag{11}$$

$$y_q(\varphi, \varphi_m, \delta) = \int g_q^{-1}(\varphi, \varphi_m, \delta) d\varphi \tag{12}$$

where, g_d^{-1} and g_q^{-1} are inverse air gap functions in polar and interpolar regions, respectively. Expression (11) is elaborated to yield

$$y_d(\varphi, \varphi_m, \delta) = \frac{1}{g_0\sqrt{1-\delta^2}} \cos^{-1}\left(\frac{\cos(\varphi - \varphi_m) - \delta}{1 - \delta\cos(\varphi - \varphi_m)}\right) \tag{13}$$

Function y_q is obtained as follows

$$\begin{aligned} y_q(\varphi, \varphi_m, \delta) &= \int \frac{1 - \beta(1 - \cos\frac{2\pi}{o'}\varphi)}{g_0(1 - \delta\cos(\varphi - \varphi_m))} d\varphi \\ &= \frac{1-\beta}{g_0} \int \frac{1}{(1 - \delta\cos(\varphi - \varphi_m))} d\varphi \\ &\quad + \frac{\beta}{g_0} \int \frac{\cos(o''\varphi)}{(1 - \delta\cos(\varphi - \varphi_m))} d\varphi \end{aligned} \tag{14}$$

where, $o'' = \frac{2\pi}{o'}$. y_q can be defined as follows

$$y_q(\varphi, \varphi_m, \delta) = \frac{1-\beta}{g_0} y_d + \frac{\beta}{g_0} y_{q1} \tag{15}$$

where, y_d is derived earlier in the paper, and y_{q1} can be obtained by some mathematical manipulations. This function is given in Appendix A.

It is assumed that functions y_1 and y_2 are the definite integrals as follows

$$y_1(\varphi_m, \theta, \delta) = \int_0^{2\pi} g^{-1}(\varphi, \varphi_m, \theta, \delta) d\varphi \tag{16}$$

$$y_2(\varphi_m, \theta, \delta) = \int_0^{2\pi} g^{-1}(\varphi, \varphi_m, \theta, \delta) n_b(\varphi) d\varphi \tag{17}$$

Separating the associated terms of polar and interpolar spaces,

(16) results in

$$y_1(\varphi_m,\theta,\delta)=\sum_{i=1}^{p}\left(\int_{\theta+(i-1)\theta_d+(i-1)\theta_q}^{\theta+i\theta_d+(i-1)\theta_q} g_d^{-1}(\varphi,\varphi_m,\delta)d\varphi + \int_{\theta+i\theta_d+(i-1)\theta_q}^{\theta+i\theta_d+i\theta_q} g_q^{-1}(\varphi,\varphi_m,\delta)d\varphi\right) \tag{18}$$

where, $\theta_q = o'$ (effective pole opening distance) and $\theta_d = \frac{2\pi}{p} - \theta_q$ in radian. Using the definitions given in (11) and (12), y_1 is obtained as follows:

$$\begin{aligned} y_1(\varphi_m,\theta,\delta)=\sum_{i=1}^{p}(&y_d(\theta+i\theta_d+(i-1)\theta_q,\varphi_m,\delta)-y_d(\theta+(i-1)\theta_d \\ &+(i-1)\theta_q,\varphi_m,\delta)+y_q(\theta+i\theta_d+i\theta_q,\varphi_m,\delta) \\ &-y_q(\theta+i\theta_d+(i-1)\theta_q,\varphi_m,\delta)) \end{aligned} \tag{19}$$

where y_d and y_q are calculated from (13) and (15), respectively. In a similar way, y_2 is calculated in the whole range of φ. Function y is defined as follows:

$$y(\varphi_m,\theta,\delta)=\frac{y_2(\varphi_m,\theta,\delta)}{y_1(\varphi_m,\theta,\delta)} \tag{20}$$

Considering (5), (16), (17) and (20), MWF of winding b, M_b is derived as

$$M_b(\varphi,\varphi_m,\theta,\delta)=n_b(\varphi)-y(\varphi_m,\theta,\delta) \tag{21}$$

To drive an expression for stator phases inductances, (21) is replaced in (4), then the associated terms of polar and interpolar regions are separated. Finally, L_{ab} is obtained as (22). The details of evaluation of L_{ab} have been given in Appendix B.

$$\begin{aligned} L_{ab}=\mu_0 lr\sum_{k=1}^{p}\Bigg[&\sum_{i=x_{2k-1}}^{i=x_{2k}} n_a(\varphi_{ti})(n_b(\varphi_{ti})-y(\varphi_m,\theta,\delta))(y_d(\varphi_{i+1},\varphi_m,\delta) \\ &-y_d(\varphi_i,\varphi_m,\delta))+\sum_{i=x_{2k}}^{i=x_{2k+1}} n_a(\varphi_{ti})\,(n_b(\varphi_{ti}) \\ &-y(\varphi_m,\theta,\delta))\,(y_q(\varphi_{i+1},\varphi_m,\delta)-y_d(\varphi_i,\varphi_m,\delta))\Bigg] \end{aligned} \tag{22}$$

In (22) $\varphi_{x_{2k-1}}$ to $\varphi_{x_{2k}}$ are the stator slots being in polar region ($\varphi_{x_{2k}} - \varphi_{x_{2k-1}} = \theta_d$) and $\varphi_{x_{2k}}$ to $\varphi_{x_{2k+1}}$ are the stator slots being in interpolar region ($\varphi_{x_{2k+1}} - \varphi_{x_{2k}} = \theta_q$).

3.2. Inductances of Rotor Windings

The procedure presented in the previous section for stator phases inductances, can be extended to rotor ones. To begin, (4) and (5) are rewritten in the rotor reference frame.

$$L_{ab} = \mu_0 lr \int_0^{2\pi} n_a(\beta) M_b(\beta, \beta_m, \delta) g^{-1}(\beta, \beta_m, \delta) d\beta \tag{23}$$

where

$$M_b(\beta, \beta_m, \delta) = n_b(\beta) - \frac{\int_0^{2\pi} g^{-1}(\beta, \beta_m, \delta).n_b(\beta) d\beta}{\int_0^{2\pi} g^{-1}(\beta, \beta_m, \delta) d\beta} \tag{24}$$

β is angle in rotor reference frame. It is assumed that the functions y_{rd} and y_{rq} to be the indefinite integral of the functions g_d^{-1} and g_q^{-1} in the rotor reference frame, respectively. Using some integration rules, y_{rd} and y_{rq} will be obtained. y_{rd} and y_{rq} are the same as y_d and y_q, but φ and φ_m are replaced with β and β_m respectively.

Equation (16) is rewritten in rotor reference frame, as follows

$$\begin{aligned}
&y_{r1}(\beta_m, \delta) \\
&= \int_0^{2\pi} g^{-1}(\beta, \beta_m, \delta) d\beta \\
&= \sum_{i=1}^{p} \left(\int_{(i-1)\theta_d + (i-1)\theta_q}^{i\theta_d + (i-1)\theta_q} g_d^{-1}(\beta, \beta_m, \delta) d\beta + \int_{i\theta_d + (i-1)\theta_q}^{i\theta_d + i\theta_q} g_q^{-1}(\beta, \beta_m, \delta) d\beta \right) \\
&= \sum_{i=1}^{p} [y_{rd}(i\theta_d + (i-1)\theta_q, \beta_m, \delta) - y_{rd}((i-1)\theta_d + (i-1)\theta_q, \beta_m, \delta) \\
&= + y_{rq}(i\theta_d + i\theta_q, \beta_m, \delta) - y_{rq}(i\theta_d + (i-1)\theta_q, \beta_m, \delta)]
\end{aligned} \tag{25}$$

where y_{rd} and y_{rq} are derived earlier in the paper. In the same way, y_{r2} can be derived.

$$y_{r2}(\beta_m, \delta) = \int_0^{2\pi} g^{-1}(\beta, \beta_m, \delta) n_b(\beta) d\beta$$

$$= \sum_{i=1}^{p} \left[\int_{(i-1)\theta_d+(i-1)\theta_q}^{i\theta_d+(i-1)\theta_q} g_d^{-1}(\beta, \beta_m, \delta) n_a(\beta) d\beta + \int_{i\theta_d+(i-1)\theta_q}^{i\theta_d+i\theta_q} g_q^{-1}(\beta, \beta_m, \delta) n_a(\beta) d\beta \right]$$

$$= \sum_{i=1}^{p} \left[n_a(\beta_{di}) \int_{(i-1)\theta_d+(i-1)\theta_q}^{i\theta_d+(i-1)\theta_q} g_d^{-1}(\beta, \beta_m, \delta) d\beta + n_a(\beta_{qi}) \int_{i\theta_d+(i-1)\theta_q}^{i\theta_d+i\theta_q} g_q^{-1}(\beta, \beta_m, \delta) d\beta \right]$$

$$\begin{aligned} = \sum_{i=1}^{p} [& n_a(\beta_{di})(y_{rd}(i\theta_d + (i-1)\theta_q, \beta_m, \delta) \\ & - y_{rd}((i-1)\theta_d + (i-1)\theta_q, \beta_m, \delta) \\ & + n_a(\beta_{qi})(y_{rq}(i\theta_d + i\theta_q, \beta_m, \delta) - y_{rq}(i\theta_d + (i-1)\theta_q, \beta_m, \delta))] \end{aligned} \quad (26)$$

where, $\beta_{di} = 2\pi(i-1)/p$ and $\beta_{di} = 2\pi(i-1)/p + \pi/4$.

M_b in rotor reference frame is defined as follows

$$M_b(\beta, \beta_m, \delta) = n_b(\beta) - \frac{y_{r2}(\beta_m, \delta)}{y_{r1}(\beta_m, \delta)} = n_b(\beta) - y_r(\beta_m, \delta) \quad (27)$$

where y_{r1} and y_{r2} are calculated from (25) and (26).

Replacing (27) in (23) and separating the associated terms of polar and interpolar regions, the expression for rotor winding inductance is derived as

$$\begin{aligned} L_{ab} = & \mu_0 lr \sum_{i=1}^{p} \left[n_a(\beta_{di})(n_b(\beta_{di}) - y_r(\beta_m, \delta)) \int_{(i-1)\theta_d+(i-1)\theta_q}^{i\theta_d+(i-1)\theta_q} g_d^{-1}(\beta, \beta_m, \delta) d\beta \right. \\ & \left. + n_a(\beta_{qi})(n_b(\beta_{qi}) - y_r(\beta_m, \delta)) \int_{i\theta_d+(i-1)\theta_q}^{i\theta_d+i\theta_q} g_q^{-1}(\beta, \beta_m, \delta) d\beta \right] \end{aligned} \quad (28)$$

$$\begin{aligned} L_{ab} = & \mu_0 lr \sum_{i=1}^{p} [n_a(\beta_{di})(n_b(\beta_{di}) - y_r(\beta_m, \delta))(y_{rd}(i\theta_d + (i-1)\theta_q, \beta_m, \delta) \\ & - y_{rd}((i-1)\theta_d + (i-1)\theta_q, \beta_m, \delta)) + n_a(\beta_{qi})(n_b(\beta_{qi}) \\ & - y_r(\beta_m, \delta))(y_{rq}(i\theta_d + i\theta_q, \beta_m, \delta) - y_{rq}(i\theta_d + (i-1)\theta_q, \beta_m, \delta))] \end{aligned}$$

where y_r and y_{rd} and y_{rq} are derived earlier in the paper.

3.3. Mutual Inductances between Stator and Rotor

For mutual inductances between rotor windings and stator phases, the stator reference frame is used. An analytical expression for mutual inductances is obtained as follows:

$$L_{ab} = \mu_0 lr \sum_{k=1}^{p} \Bigg[n_a(\beta_{di}+\theta) \sum_{i=x_{2k-1}}^{i=x_{2k}} \big[(n_b(\varphi_{ti}) - y(\varphi_m,\theta,\delta))(y_d(\varphi_{i+1},\varphi_m,\delta) - y_d(\varphi_i,\varphi_m,\delta))\big] + n_a(\beta_{qi}+\theta) \sum_{i=x_{2k}}^{i=x_{2k+1}} [(n_b(\varphi_{ti}) - y(\varphi_m,\theta,\delta))(y_q(\varphi_{i+1},\varphi_m,\delta) - y_q(\varphi_i,\varphi_m,\delta))] \Bigg] \quad (29)$$

where a and b are accounted for the rotor windings and stator phases, respectively. Functions y, y_d and y_q are defined earlier in the paper.

Therefore, the inductances of SPSM under different kinds of eccentricities can be calculated in a unified technique by means of (22), (28) and (29). In the presented analytical expressions, unlike previous proposals, effective form of pole shoes considering flux fringing effect is taken into account.

4. COMPUTATION OF INDUCTANCES

In this section, by means of developed analytical expressions, inductances of a SPSM for healthy and different eccentricity conditions are calculated in a unified technique, where the eccentricity type and degree are selectable. A typical SPSM, with specifications given in Appendix C, is considered in this paper. It should be noted that, magnetic saturation and leakage flux are not included.

4.1. Magnetizing and Mutual Inductances of Stator Phases

Magnetizing inductance of stator phase a and mutual inductance between phases a and b of the stator have been computed under different eccentricity conditions and are shown in Figures 4 and 5.

Comparison of plots in Figures 4 and 5 for the three types of eccentricity shows that while ME causes asymmetrical self and mutual inductances, SE and DE cause symmetrical inductances. By increasing the eccentricity severity, the magnitude of these inductances increases.

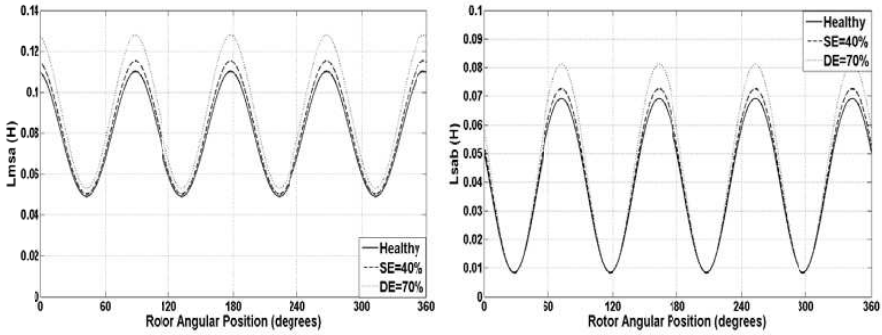

Figure 4. Calculated inductances of stator phases versus rotor position under healthy and different eccentricity conditions, (a) magnetizing inductance of stator phase a, and (b) mutual inductance between phases a and b of the stator.

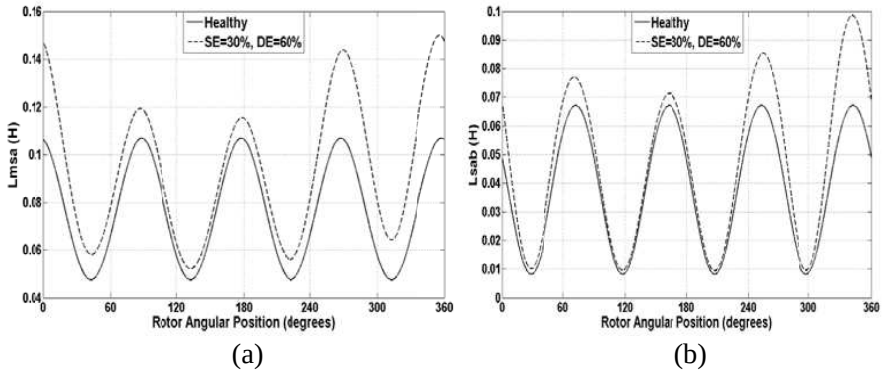

Figure 5. Calculated inductances of stator phases versus rotor position under healthy and ME conditions (SE = 30%, DE = 60%), (a) magnetizing inductance of stator phase a, and (b) mutual inductance between phases a and b of the stator.

4.2. Magnetizing Inductance of Rotor Winding

The plots of magnetizing inductance of rotor winding for different eccentricities are shown in Figure 6. Comparison of plots in Figure 6 shows how SE, DE and ME affect the profile of the magnetizing inductance of rotor winding. ME causes a pulsating magnetizing inductance of rotor winding, whereas, DE and SE cause a symmetrical inductance with a larger magnitude compared to the non-eccentric

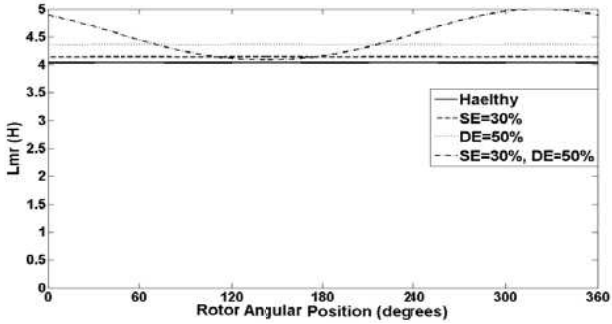

Figure 6. Calculated magnetizing inductance of rotor winding versus rotor position, under healthy and different eccentricity conditions.

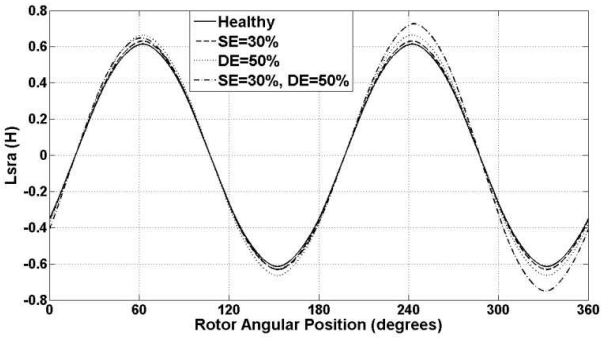

Figure 7. Calculated mutual inductance between stator phase a and rotor winding under different eccentricity conditions.

condition. By increasing the eccentricity level, the magnitude of this inductance increases.

4.3. Mutual Inductances between Stator Phases and Rotor Winding

Figure 7 shows the mutual inductance between stator phase a and rotor winding for different eccentricity cases.

Comparison of the inductance profiles in Figure 7 indicates that SE and DE increase the magnitude of mutual inductance whereas there is no asymmetry in the inductance distribution and ME creates asymmetrical inductance distribution.

5. EXPERIMENTAL RESULTS

To validate the theoretical and simulated results, experiments were performed on a machine identical to the one simulated. A technique was used to make the machine temporarily eccentric with different types and degrees of eccentricities. The stator and the rotor bearings at the two ends of the motor were separately mounted on the test bed. Therefore, it was possible to displace any of bearings separately and create different static eccentricities. To be able to create dynamic eccentricity, bearings were replaced by other bearings with different diameter. Special screws were used to fix the bearings. The position of bearings was accurately checked by a clock. The clock and special screw are shown in Figure 8.

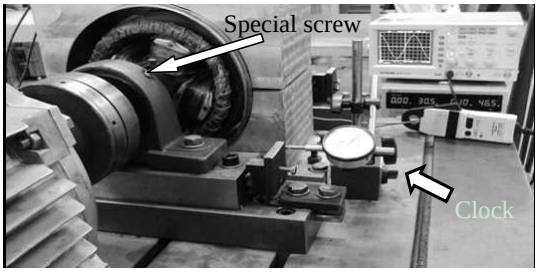

Figure 8. Test bed.

To obtain the mutual inductance between stator phase a and stator phase b, a sinusoidal voltage was applied in stator phase a and the voltage induced in the stator phase b was measured as a function of the rotor position from 0° to 360° taking 3° steps. The mutual inductance was calculated as follows:

$$L_{ab}(\theta) = \frac{V_b(\theta)}{V_a(\theta)} L_{aa}(\theta) \tag{30}$$

where $V_a(\theta)$ and $V_b(\theta)$ are induced voltages in stator phase a and stator phase b, respectively and $L_{aa}(\theta)$ is self inductance of stator phase a, previously calculated by means of phase a voltage and current measurements.

The induced voltage in phase A was derived as follows:

$$V_A = \sqrt{V_s^2 - (r_A i_A)^2} \tag{31}$$

where V_s is the applied voltage, i_A is the current following in stator phase A and r_A is stator phase A resistance (1.36 Ω). To avoid the

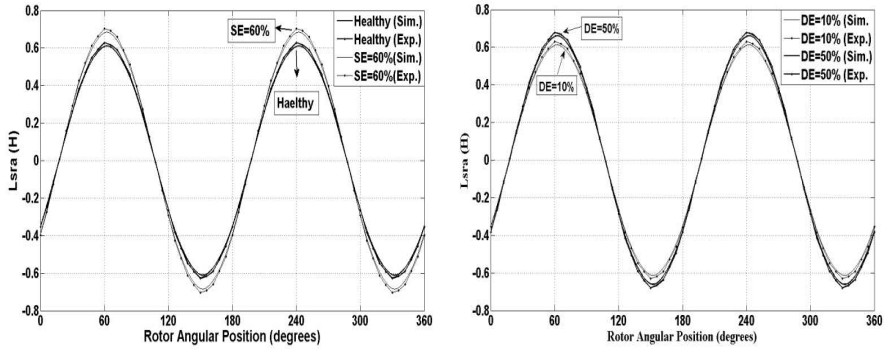

Figure 9. Mutual inductance between stator phase a and rotor winding under healthy and different eccentricities for the experiment and simulation.

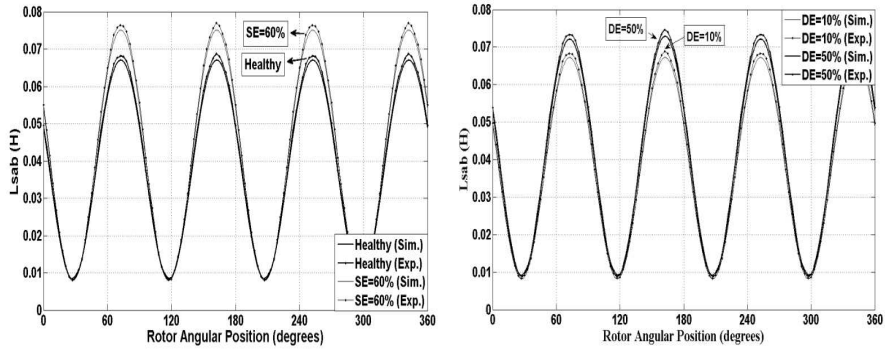

Figure 10. Mutual inductance between stator phase a and stator phase b under healthy and different eccentricities for the experiment and simulation.

magnetic saturation, a low ac voltage was applied. The phase A voltage drop was negligible in the experiments.

The mentioned process was repeated to obtain the mutual inductance between stator phase a and rotor winding.

Figures 9 and 10 show the profiles of mutual inductances under eccentricity conditions for the experiment and simulation. It is apparent that the inductance profiles coming from the simulation and experiment demonstrate a satisfactory mach. The reasons of this agreement are as follows: 1) a more realistic distribution of the air

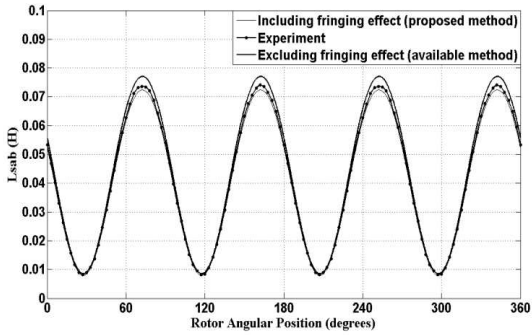

Figure 11. Calculated mutual inductance between stator phase a and phase b, for machine under 50% static eccentricity from proposed analytical method, available analytical method and experiment.

gap in the presence of eccentricity considering flux fringing effect is used, 2) development in Fourier series of the inverse air gap function has not been used, but closed form analytical equations are employed for inductances calculation and 3) real spatial distribution of stator phases and rotor winding has also been taken into account.

Figure 11 shows the mutual inductance between stator phase a and phase b for machine under 50% static eccentricity from simulations and experiment. The inductance was calculated using proposed analytical method and available analytical method in which, the air gap function is estimated by a step function. The comparison between inductance profiles indicates that the maximum value of the inductance from the proposed method is slightly lower than the available method result. The main reason is that in the proposed method the flux fringing effect is considered, while in previous analytical method, based on winding function theory, this effect is excluded.

As shown, the result with proposed method is closer to the experimental result than that of available method. Probably, the difference between results from the proposed method and the experiment is due to neglecting the slots flux leakages. This claim needs more detailed study.

6. CONCLUSIONS

In this study, a new analytical model for SPSM under general eccentricity fault has been developed, capable of accounting for the machine geometry, effect of flux fringing, slots effect and spatial distribution of machine windings. While in previous analytical

methods, air gap function has been estimated and therefore geometrical model has been simplified, in this paper, effective air gap function which considers flux fringing effect is taken into account.

By using the effective air gap function of the eccentric SPSM and determining its indefinite integral, precise analytical equations for inductances have been obtained. Derived comprehensive equations allow calculating time varying inductances of SPSM under any eccentricity type and degree, with a general simulation technique. Analytical equations prevent imprecision due to numerical differentiations. Moreover, the computational time is decreased thanks to an exact and analytical definition of the distribution functions, in contrast to methods based on only an approximation with Fourier series.

Simulation results show that the result with the proposed method is closer to the experimental result than that of available analytical methods. The main reason is that in the proposed method the flux fringing effect is considered, while in previous analytical method, based on winding function theory, this effect is excluded and the air gap distribution is estimated by step function. Since the calculation of inductances is an essential step for simulation and analysis of fault in electrical machines, the proposed method will improve the on-line diagnosis of the fault. The author plans to apply the evaluated inductances in a coupled electromagnetic model of SPSM in the future for fault analysis.

ACKNOWLEDGMENT

This work was supported by the Office of Vice Chancellor for Research, Yazd Branch, Islamic Azad University, Yazd, Iran. The author would like to thank Dr. H. Meshgin Kelk for providing information regarding the installed 9 KVA synchronous machine in the electrical machines research Lab, Tafresh University, Iran and Prof. J. Milimonfared from Amirkabir University of technology, Tehran, Iran.

APPENDIX A.

$$
\begin{aligned}
& y_{q1} \\
&= -\frac{\left[(o''/2)\delta^4-(o''\delta)^2+o''^2\right]\cos(o''\phi_m)}{\delta^4\sqrt{\delta^2-1}}\tanh^{-1}\left(\frac{\delta+1}{\sqrt{\delta-1}}\tan\left(\frac{\phi-\phi_m}{2}\right)\right) \\
&\quad +\frac{o''\delta^2-2o''}{\delta^4}\left[(\phi-\phi_m)\cos(o''\phi_m)+\sin(o''\phi_m)\ln\left(1-\delta\cos\left(\phi-\phi_m\right)\right)\right] \\
&\quad -\frac{2}{\delta^2}\sin(2\phi+2\phi_m)-\frac{2}{3\delta}\sin(3\phi+\phi_m)+\frac{2\delta^2-2o''}{\delta^3}\sin(\phi+3\phi_m) \\
&\quad f_q(\varphi,\varphi_m,\delta) \\
&= \frac{1-\beta}{g_0}\int\frac{1}{(1-\delta\cos(\varphi-\varphi_m))}d\varphi+\frac{\beta}{g_0}\int\frac{\cos\frac{2\pi}{o'}\varphi}{(1-\delta\cos(\varphi-\varphi_m))}d\varphi.
\end{aligned}
$$

APPENDIX B.

Replacing (21) in (4) and separating the associated terms of polar and interpolar regions, L_{ab} is obtained as follows:

$$
\begin{aligned}
L_{ab} = \mu_0 lr\sum_{i=1}^{p}\Bigg[& \int_{\theta+(i-1)\theta_d+(i-1)\theta_q}^{\theta+i\theta_d+(i-1)\theta_q} g_d^{-1}(\varphi,\varphi_m,\theta,\delta)n_a(\varphi)(n_b(\varphi) \\
& -y(\varphi_m,\theta,\delta))d\varphi+\int_{\theta+i\theta_d+(i-1)\theta_q}^{\theta+i\theta_d+i\theta_q} g_q^{-1}(\varphi,\varphi_m,\theta,\delta)n_a(\varphi)(n_b(\varphi) \\
& -f(\varphi_m,\theta,\delta))d\varphi\Bigg]
\end{aligned}
\tag{B1}
$$

where a and b are accounted for the stator phases. It is assumed that $\varphi_{x_{2k-1}}$ to $\varphi_{x_{2k}}$ are the stator slots being in polar region ($\varphi_{x_{2k}}-\varphi_{x_{2k-1}}=\theta_d$) and $\varphi_{x_{2k}}$ to $\varphi_{x_{2k+1}}$ are the stator slots being in interpolar region ($\varphi_{x_{2k+1}}-\varphi_{x_{2k}}=\theta_q$). Therefore

$$
\begin{aligned}
L_{ab}=\mu_0 lr\sum_{k=1}^{p}\Bigg[& \sum_{i=x_{2k-1}}^{i=x_{2k}} n_a(\varphi_{ti})(n_b(\varphi_{ti})-f(\varphi_m,\theta,\delta))\int_{\varphi_i}^{\varphi_{i+1}} g_d^{-1}(\varphi,\varphi_m,\delta)d\varphi \\
& +\sum_{i=x_{2k}}^{i=x_{2k+1}} n_a(\varphi_{ti})(n_b(\varphi_{ti})-f(\varphi_m,\theta,\delta))\int_{\varphi_i}^{\varphi_{i+1}} g_q^{-1}(\varphi,\varphi_m,\delta)d\varphi\Bigg]
\end{aligned}
\tag{B2}
$$

where φ_i is angle of stator slot i center, φ_{ti} is angular position between stator slot i and stator slot $i+1$ (angle of stator tooth i). $\varphi_{x_{2k-1}}$, $\varphi_{x_{2k}}$ and $\varphi_{x_{2k+1}}$ can be easily determined at every time step of simulation. Using the definitions given in (11) and (12), L_{ab} is obtained as (22).

APPENDIX C.

Table C1. Specifications of simulated machine.

Pole arc (degrees)	57
Inner radius of stator (mm)	80
Air gap length (mm)	0.6
Active axial length (mm)	130
Number of turns per slot	20
Number of stator slots	30
Stator slot pitch (degrees)	12
Rotor outer radius (mm)	79.4

REFERENCES

1. Toliyat, H., T. A. Lipo, and J. C. White, "Analysis of a concentrated winding induction machine for adjustable speed drive applications. I. Motor analysis," *IEEE Transactions on Energy Conversion*, Vol. 6, 679–692, 1991.
2. DeBortoli, M. J., S. J. Salon, and C. J. Slavic, "Effect of rotor eccentricity and parallel winding on induction behavior: A study using finite element analysis," *IEEE Transactions on Magnetics*, Vol. 29, No. 2, 1676–1682, 1993.
3. Vaseghi, B., N. Takorabet, and F. Meibody-Tabar, "Transient finite element analysis of induction machines with stator winding turn fault," *Progress In Electromagnetics Research*, Vol. 95, 1–18, 2009.
4. Milimonfared, J., H. Meshgin Kelk, A. Der Minassians, S. Nandi, and H. A. Toliyat, "A novel approach for broken bar detection in cage induction motors," *IEEE Transactions on Industry Applications*, Vol. 35, 1000–1006, 1999.
5. Joksimovic, M. G. and J. Penman, "The detection of inter turn short circuits in the stator windings of operating motors", *IEEE Transactions on Industry Application*, Vol. 47, 1078–1084, 2000.

6. Al-Nuaim, N. A. and H. Toliyat, "A novel method for modeling dynamic air-gap eccentricity in synchronous machines based on modified winding function theory," *IEEE Transactions on Energy Conversion*, Vol. 13, 156–162, 1998.
7. Tabatabaei, I, J. Faiz, H. Lesani, and M. T. Nabavi-Razavi, "Modeling and simulation of a salient pole synchronous generator with dynamic eccentricity using modified winding function approach," *IEEE Transactions on Magnetics*, Vol. 40, No. 3, May 2004.
8. Joksimovic, G. M., "Dynamic simulation of cage induction machine with air gap eccentricity," *IEE Proc. Electr. Power Appl.*, Vol. 152, No. 4, 803–811, July 2005.
9. Mishra, C., A. Routray, and S. Mukhopadhyay, "A computationally efficient winding function method for calculation of inductances in an asymmetric induction motor," *Electric Power Components and Systems*, Vol. 35, No. 1, 43–61, 2007.
10. Akbari, H., H. Meshgin Kelk, and J. Milimonfared, "Extension of winding function theory for radial and axial non-uniform air gap in salient pole synchronous machines," *Progress In Electromagnetics Research*, Vol. 114, 407–428, 2011.
11. Lubin, T. and T. Hamiti, H. Razik, and A. Rezzoug, "Comparison between finite element analysis and winding function theory for inductances and torque calculation of a synchronous reluctance machine," *IEEE Transactions on Magnetics*, Vol. 43, No. 8, 3406–3410, 2007.
12. Babaei, M., J. Faiz, B. M. Ebrahimi, S. Amini, and J. Nazarzadeh, "A detailed analytical model of a salient-pole synchronous generator under dynamic eccentricity fault," *IEEE Transactions on Magnetics*, Vol. 47, No. 4, 64–771, 2011.
13. Toliyat, H. A. and N. A. Al-Nuaim, "Simulation and detection of dynamic air-gap eccentricity in salient-pole synchronous machines," *IEEE Transactions on Industry Applications*, Vol. 35, No. 1, 86–93, 1999.
14. Tu, X., L.-A. Dessaint, M. El Kahel, and A. Barry, "Modeling and experimental validation of internal faults in salient pole synchronous machines including space harmonics," *Mathematics and Computers in Simulation*, Vol. 71, 425–439, 2006.
15. Neti, P. and S. Nandi, "Stator interturn fault detection of synchronous machines using field current and rotor search-coil voltage signature analysis," *IEEE Transactions on Industry Applications*, Vol. 45, No. 3, 911–920, 2009.
16. Dehkordi, A., P. Neti, A. Gole, and T. Maguire, "Development

and validation of a comprehensive synchronous machine model for a real time environment," *IEEE Transactions on Energy Conversion*, Vol. 25, No. 1, 34–48, 2010.

17. Akbari, H., J. Milimonfared, and H. Meshgin Kelk, "A novel technique for the computation of inductances of salient pole machines under different eccentricity conditions," *Electric Power Components and Systems*, Vol. 39, No. 14, 1507–1522, 2011.
18. Faiz, J., I. Tabatabaei, and E. Sharifi, "A precise electromagnetic modeling and performance analysis of a three-phase squirrel-cage induction motor under mixed eccentricity condition," *Electromagnetics*, Vol. 24, 471–489, 2004.
19. Ostovic, V., *Computer Aided Analysis of Electrical Machines, A Mathematical Approach,* Prentice Hall, Englewood Cliffs, NJ, 1994.
20. Akbari, H., "Analytical computation of reluctance synchronous machine inductances under different eccentricity faults," *Progress In Electromagnetics Research M*, Vol. 24, 29–44, 2012.